



HAL
open science

Broadcasting in Cognitive Radio Networks: A Fountain Codes Approach

Lam-Thanh Tu, Tan Nguyen, Tran Trung Duy, Phuong Tran, Miroslav Voznak, Alexis I Aravanis

► **To cite this version:**

Lam-Thanh Tu, Tan Nguyen, Tran Trung Duy, Phuong Tran, Miroslav Voznak, et al.. Broadcasting in Cognitive Radio Networks: A Fountain Codes Approach. *IEEE Transactions on Vehicular Technology*, 2022, 71 (10), pp.11289-11294. 10.1109/TVT.2022.3188969 . hal-04113437

HAL Id: hal-04113437

<https://hal.science/hal-04113437v1>

Submitted on 1 Jun 2023

HAL is a multi-disciplinary open access archive for the deposit and dissemination of scientific research documents, whether they are published or not. The documents may come from teaching and research institutions in France or abroad, or from public or private research centers.

L'archive ouverte pluridisciplinaire **HAL**, est destinée au dépôt et à la diffusion de documents scientifiques de niveau recherche, publiés ou non, émanant des établissements d'enseignement et de recherche français ou étrangers, des laboratoires publics ou privés.

Broadcasting in Cognitive Radio Networks: A Fountain Codes Approach

Lam-Thanh Tu, Tan N. Nguyen, *Member, IEEE*, Tran Trung Duy, Phuong T. Tran, *Senior Member, IEEE*, Miroslav Voznak, *Senior Member, IEEE* and Alexis I. Aravanis

Abstract—The present paper addresses the performance of the broadcasting scheme in cognitive radio networks (CRNs) under a fountain codes (FC) approach. Particularly, closed-form expressions are derived for the cumulative distribution function (CDF) and the expectation of the number of FC clock cycles required for broadcasting packets to all secondary receivers. The energy efficiency (EE) of the secondary networks (SN) is also provided. Moreover, a simple transmit power scheme is proposed to enhance the performance of the SN and guarantee the quality-of-service (QoS) of the primary network (PN). The trends of the introduced closed-form performance metrics are then examined versus important network parameters allowing for the optimization of those parameters. Finally, numerical results are provided to confirm the accuracy of the derived mathematical framework and the superior performance of the introduced FC scheme over uncoded broadcasting protocols.

Index Terms—Broadcasting, cognitive radio, fountain codes, performance analysis.

I. INTRODUCTION

Cognitive radio networks (CRNs) has emerged as a solution to increase the utilization of the scarce licensed spectrum by allowing secondary users (SUs) to operate alongside primary users (PUs), over the same resources in the frequency, time and spatial domain. Among all available protocols, i.e., overlay, interweave and underlay protocols, the underlay protocol gains lots of attention from both academia and industry since it allows the SUs to operate concurrently with the PUs providing that the aggregate SUs interference at the PUs remains under a predefined threshold [1].

Another solution that has been used extensively to ameliorate the transmission efficiency of current networks is the employment of Fountain codes (FC) (a.k.a rateless codes) [2]. FC multiply the packets to be transmitted, with the elements of a (different at each clock cycle) random generator matrix and subsequently sum bitwise the elements of this

product. This gives rise to a different encoded packet per clock cycle. Receivers can successfully decode the original message after receiving a sufficient number of these different encoded packets. Thus, FCs can adapt to adverse channel conditions and obviate the need for sharing the channel state information (CSI) at the transmitter. There were a few works studying the impact of FCs on the CRNs environments [3], [4]. Particularly, the resource optimization problem at the multiuser MIMO feedback channel, under imperfect CSI at the transmitter, has been investigated for a FC CRNs in [3]; while the average throughput and transmission time of dual-hop overlay FC CRNs is examined in [4]. Both works highlight the benefits arising from employing FC in CRNs.

Building upon these documented benefits, the present letter investigates the potential of employing FCs to address one of the fundamental challenges of CRNs, that is the broadcasting of packets in the network. Broadcasting is vital but extremely challenging in CRNs due to the heterogeneous spectrum availability [5]. In this course, the present letter employs FC to facilitate the broadcasting of packets in CRNs and provides an analytical framework for optimizing the network parameters toward guaranteeing the success of the broadcasting.

To elaborate, the present letter i) derives in a closed-form the energy efficiency (EE) of the secondary networks (SN) as well as the cumulative distribution function (CDF) and the expectation of the number of clock cycles that allow for the successful broadcasting of all necessary packets to all SUs ii) examines the trends of the CDF with respect to key network parameters, namely, the transmit power of the primary transmitter, the number of transmitted packets and secondary receivers (SRs); thus allowing for the optimization of the respective parameters; iii) introduces a simple transmit power scheme that guarantees the quality-of-service (QoS) of the primary network; iv) compares the introduced FC scheme versus a benchmark uncoded broadcast (UB) protocol¹, by introducing a mathematical framework for the latter protocol, demonstrating the superior performance of the introduced FC broadcasting scheme.

II. SYSTEM MODEL

The considered CRN comprises one secondary transmitter ST and \mathcal{K} secondary receivers SR_k , $k \in \{1, \dots, \mathcal{K}\}$ in the secondary network, as shown in Fig. 1. We assume that ST is located at the origin of the two-dimensional plane and the SRs are distributed around the ST and known to the ST via localization techniques. The primary network² (PN)

¹The UB scheme is chosen as the benchmark, since it employs a re-transmission protocol like any other error correcting code (ECC) to correct erroneous packets, however, it does not require additional redundant bits and has therefore the same packet length as the considered scheme.

²The primary network can be considered the cellular network.

Manuscript received Jan., 2022; revised May, 2022; accepted Jun. 2022; this work was supported in part by the Ministry of Education, Youth and Sport of the Czech Republic under the grant SP2021/25, the H2020 MSCA IF Pathfinder project under grant agreement 891030 and by Vietnam National Foundation for Science and Technology Development (NAFOSTED) under grant number 102.04-2021.57. Copyright (c) 2015 IEEE. Personal use of this material is permitted. However, permission to use this material for any other purposes must be obtained from the IEEE by sending a request to pubpermissions@ieee.org. (*Corresponding author: Tan N. Nguyen*)

Lam-Thanh Tu and Tan N. Nguyen are with the Communication and Signal Processing Research Group, Faculty of Electrical and Electronics Engineering, Ton Duc Thang University, 756000 Ho Chi Minh City, Vietnam (email: {tulamthanh, nguyennhattan}@tdtu.edu.vn).

Phuong T. Tran is with the Wireless Communications Research Group, Faculty of Electrical and Electronics Engineering, Ton Duc Thang University, 756000 Ho Chi Minh City, Vietnam (email: tranthanhphuong@tdtu.edu.vn).

Tran Trung Duy is with the Posts and Telecommunications Institute of Technology, Ho Chi Minh City, Vietnam (email: trantrungduy@ptithcm.edu.vn).

Miroslav Voznak is with VSB – Technical University of Ostrava, 70800 Ostrava, Czech Republic. (e-mail: miroslav.voznak@vsb.cz).

Alexis I. Aravanis is with Université Paris-Saclay, CNRS, CentraleSupélec, L2S, 91192 Gif-sur-Yvette, France. (alexis.aravanis@centralesupelec.fr).

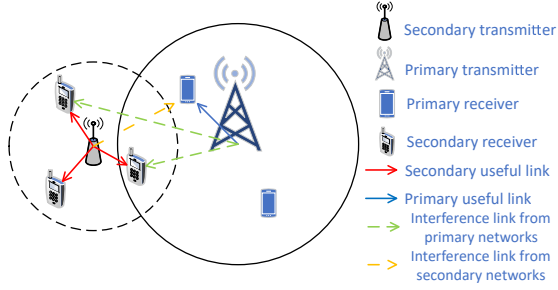


Fig. 1. System model of the considered cognitive radio network.

TABLE I: Notation and mathematical symbols

Symbol	Definition
$\mathbb{E}\{\cdot\}, \Pr(\cdot)$	Expectation & Probability operators
max, min	Maximum and minimum function
$\log, \text{B}(\cdot, \cdot)$	Logarithm and beta function
$\mathcal{I}_x(a, b)$	Regularized incomplete beta function
$d_{u,v}$	Euclidean distance from u to v
$\omega_{u,v}$	Large-scale path-loss from u to v
$h_{u,v}^{(\tau)}$	Channel coefficient from u to v at τ time-slot
P_P, P_S	Transmit power of PT and ST
K_0, η	Path-loss constant and path-loss exponent
R_P, R_S	Expected rate of primary & secondary networks
\mathcal{K}, \mathcal{G}	Number of secondary receivers and packets
n_k, σ_k^2	AWGN noise and its variance at k -th SR
$x^{(\tau)}, x_P^{(\tau)}$	Transmit signals of ST and PT
NF, BW	Noise figure and transmission bandwidth
P_{\max}	Maximum transmission power of ST
σ_P^2	Noise variance of PR
v	Pre-defined OP target of primary networks
$\mathcal{E}_X(\mathcal{G})$	Mean of required time-slot under X scheme
$F_X(x), f_X(x)$	CDF and PDF of RV X
$P_{\text{suc}}(\gamma_S)$	Probability to successfully receive a packet

includes a transmitter and a receiver denoted by PT and PR. The ST broadcasts a common message of \mathcal{G} packets, e.g., a safety warning, a weather forecast, etc., to all \mathcal{K} SRs employing the underlay protocol. The ST keeps transmitting until receiving acknowledgement (ACK) packets from all \mathcal{K} SRs indicating that the message has been successfully delivered. We assume that the ST transmits a packet per clock cycle. The injecting marker technique is employed to ensure the same packet lengths between the primary and secondary networks. Additionally, the time-slotted medium access control (MAC) protocol is adopted. We also assume a simple high-accuracy feedback channel between all SRs and ST so that all single-bit ACK messages are successfully decoded by the ST. Besides, the ST has perfect CSI of the primary network by employing the spectrum sensing, database, and SNR estimation techniques [1]. Two different broadcasting schemes are employed to send packets to SRs.

- 1) *Fountain Codes Broadcast (FCB)*: The system employs FC to encode the message. At each time slot (i.e. clock cycle), the ST transmits a new FC encoded packet. After successfully receiving \mathcal{G} packets, each receiver transmits an ACK message to announce to the ST the successful transmission.
- 2) *Uncoded Broadcast (UB)*: Under this scheme, the ST transmits the same packet until the ACK packets from all SRs are received by the ST. Once all ACK packets are

received, the ST starts transmitting a new packet until all \mathcal{G} packets are successfully delivered to all SRs.

The received signal by the k -th SRs at the τ -th clock cycle (i.e. time-slot) is denoted by $y_k^{(\tau)}$ is given by

$$y_k^{(\tau)} = \sqrt{P_S \omega_{ST,SR_k}} h_{ST,SR_k}^{(\tau)} x^{(\tau)} + \sqrt{P_P \omega_{PT,SR_k}} h_{PT,SR_k}^{(\tau)} x_P^{(\tau)} + n_k. \quad (1)$$

Here P_P and P_S is the transmit power of the PT and ST; $h_{u,v}^{(\tau)}$ is the channel coefficient from transmitter $u \in \{\text{ST}, \text{PT}\}$ to receiver $v \in \{\text{SR}_k, \text{PR}\}$, $k \in \{1, \dots, \mathcal{K}\}$ at the $\tau \in \mathbb{N}$ time-slot and follows a complex Gaussian distribution with zero mean and $\lambda_{u,v}$ variance³, i.e., $h_{u,v} \sim \mathcal{CN}(0, \lambda_{u,v})$; $\omega_{u,v} = K_0 (1 + d_{u,v})^{-\eta}$ [6] is the large-scale path-loss from u to v ; $d_{u,v}$ is the distance from u to v ; $K_0 = (4\pi f_c/c)^{-2}$ and $\eta > 2$ are the path-loss constant and the path-loss exponent, respectively; f_c is the carrier frequency (in Hz) and $c = 3 \times 10^8$ (in meters per second) is the speed of light; n_k is the AWGN noise of SR $_k$; $x^{(\tau)}$ and $x_P^{(\tau)}$ are the signals transmitted from ST and PT at the τ -th time-slot and $\mathbb{E}\{|x^{(\tau)}|^2\} = \mathbb{E}\{|x_P^{(\tau)}|^2\} = 1$. $\mathbb{E}\{\cdot\}$ is the expectation operator. Table I provides main notations and mathematical symbols of the paper. The signal-to-interference-plus-noise ratio (SINR) of the k -th SR at the τ -th time-slot is then given by

$$\text{SINR}_k^{(\tau)} = P_S \omega_{ST,SR_k} |h_{ST,SR_k}^{(\tau)}|^2 / \left(\sigma_k^2 + P_P \omega_{PT,SR_k} |h_{PT,SR_k}^{(\tau)}|^2 \right), \quad (2)$$

where σ_k^2 is the noise variance for SR $_k$. We assume that $\sigma_k^2 = \sigma^2 = -174 + \text{NF} + 10 \log(\text{Bw}) \forall k$; where NF (in dB) is the noise figure; and Bw (in Hz) is the transmission bandwidth. We consider the worst case scenario where the SRs always suffer from the interference created by the PT. Since the fast fading does not explicitly depend on the time-slot but is rather given by the assumed distribution, the superscripts τ in (2) are omitted and (2) is re-written as:

$$\text{SINR}_k = P_S \omega_{ST,SR_k} |h_{ST,SR_k}|^2 / \left(\sigma_k^2 + P_P \omega_{PT,SR_k} |h_{PT,SR_k}|^2 \right). \quad (3)$$

III. PERFORMANCE ANALYSIS AND TRENDS

In this section, we derive the mean and the CDF of the clock cycles required for broadcasting \mathcal{G} packets to \mathcal{K} SRs under both the FCB and the UB protocols. We also compute the probability of a SR to successfully receive a packet. In this course, we employ the following Lemma.

Lemma 1: Given two independent exponential random variables (RVs) X and Y with corresponding parameters ω_X and ω_Y and three real positive numbers $a, b, c > 0$. The complementary cumulative distribution function (CCDF) of the RV $Z = aX/(c + bY)$, denoted by $\bar{F}_Z(z)$, is given by

$$\begin{aligned} \bar{F}_Z(z) &= \Pr \{ aX / (c + bY) \geq z \} \\ &= \exp(-zc / (a\omega_X)) (1 + zb\omega_Y / (a\omega_X))^{-1}. \end{aligned} \quad (4)$$

Here $\Pr \{\cdot\}$ is the probability operator.

Proof: The proof is available in Appendix A. \blacksquare

A. Transmit power of secondary transmitters

To guarantee the QoS of the PN, and that the outage probability (OP) denoted by OP_{PR} will be below the pre-

³Rayleigh fading is applied due to its mathematical tractability and its worse case performance compared to other fading distributions.

determined target, i.e., $\text{OP}_{\text{PR}} \leq v$, $v \in (0, 1]$, a simple transmit power scheme is employed at the ST:

$$P_{\text{S}} = \begin{cases} \min \{ [P_{\text{adp}}]^+, P_{\text{max}} \} & P_{\text{P}} > 0 \\ P_{\text{max}} & P_{\text{P}} = 0 \end{cases} \quad (5)$$

$$P_{\text{adp}} = C_4 P_{\text{P}} (\exp(-C_3/P_{\text{P}}) (1-v)^{-1} - 1).$$

Here $C_3 = \gamma_{\text{P}} \sigma_{\text{P}}^2 / \Omega_{\text{PT,PR}}$, $C_4 = \Omega_{\text{PT,PR}} / (\Omega_{\text{ST,PR}} \gamma_{\text{P}})$, $\Omega_{u,v} = \omega_{u,v} \lambda_{u,v}$, σ_{P}^2 is the PR noise variance; R_{P} is the expected rate of the PN, $\gamma_{\text{P}} = 2^{R_{\text{P}}} - 1$, $[x]^+ = \max\{x, 0\}$ and P_{max} is the maximum transmission power of the ST. From (5), we observe that the complexity to obtain P_{adp} is approximately $O(\log^2 n)$ [7].

Proof: The proof is given in Appendix B. ■

The main benefit of the adopted transmit power policy is that it maximizes the performance of the secondary network while guaranteeing the QoS of the primary network.

B. Probability to successfully receive a packet at the SRs

The probability of SR_k to successfully receive a packet is denoted by $P_{\text{suc}_k}(\gamma_{\text{S}})$ and is given by the probability of the SINR at SR_k to be greater than the pre-defined threshold, $\gamma_{\text{S}} = 2^{R_{\text{S}}} - 1$. Hence, $P_{\text{suc}_k}(\gamma_{\text{S}})$ is given by

$$P_{\text{suc}_k}(\gamma_{\text{S}}) = \Pr \{ \log_2(1 + \text{SINR}_k) \geq R_{\text{S}} \} = \Pr \{ \text{SINR}_k \geq \gamma_{\text{S}} \} \\ = \exp(-C_{1,k}/P_{\text{S}}) (1 + C_{2,k}P_{\text{P}}/P_{\text{S}})^{-1}, \quad (6)$$

where $C_{1,k} = \gamma_{\text{S}} \sigma^2 / \Omega_{\text{ST,SR}_k}$, $C_{2,k} = \gamma_{\text{S}} \Omega_{\text{PT,SR}_k} / \Omega_{\text{ST,SR}_k}$, R_{S} is the expected rate of the secondary network.

Proof: (6) holds by combining (3) and Lemma 1. ■

C. CDF of clock cycles required for broadcasting under FCB

The CDF of the clock cycles required for broadcasting \mathcal{G} packets under the FCB scheme is denoted by $F_{T_{\text{FCB}}}(t_{\text{FC}}, \mathcal{G})$:

$$F_{T_{\text{FCB}}}(t_{\text{FC}}, \mathcal{G}) = \Pr \{ T_{\text{FCB}} \leq t_{\text{FC}} \} \\ = \prod_{k=1}^{\mathcal{K}} \mathcal{I}_{P_{\text{suc}_k}(\gamma)}(\mathcal{G}, t_{\text{FC}} - \mathcal{G} + 1), \quad (7)$$

where $\mathcal{I}_x(a, b)$ is the regularized incomplete beta function [8, 8.392].

Proof: The proof is available in Appendix C. ■

D. Mean of clock cycles required for broadcasting under FCB

The average number of clock cycles for broadcasting \mathcal{G} packets under FCB scheme is denoted by $\mathcal{E}_{\text{FCB}}(\mathcal{G})$:

$$\mathcal{E}_{\text{FCB}}(\mathcal{G}) = \mathbb{E} \{ T_{\text{FCB}} \} = \sum_{x=\mathcal{G}}^{\infty} x \Pr \{ T_{\text{FCB}} = x \} \\ \stackrel{(a)}{=} \sum_{x=\mathcal{G}}^{\infty} \sum_{i_1=1}^{\mathcal{K}} \cdots \sum_{i_{\mathcal{K}}=1}^{\mathcal{K}} x \left(\prod_{k=1}^{\mathcal{K}} \mathcal{A}_{k,i_k}(x) \right), \quad (8)$$

where $\mathcal{A}_{k,1}(x) = \mathcal{I}_{P_{\text{suc}_k}(\gamma_{\text{S}})}(\mathcal{G}, x - \mathcal{G})$; $\mathcal{A}_{k,2}(x) = \frac{(P_{\text{suc}_k}(\gamma_{\text{S}}))^{\mathcal{G}} (1 - P_{\text{suc}_k}(\gamma_{\text{S}}))^{x-\mathcal{G}}}{(x-\mathcal{G})\text{B}(\mathcal{G}, x-\mathcal{G})}$ and $\sum = \underbrace{\sum_{i_1=1}^{\mathcal{K}} \cdots \sum_{i_{\mathcal{K}}=1}^{\mathcal{K}}}_{\forall i_k \in \{1, 2\} \setminus \{i_1 = \dots = i_{\mathcal{K}} = 1\}}$;

$\text{B}(\cdot, \cdot)$ is the Beta function [8, 8.380.1]; and (a) holds by employing [9, 8.17.21].

Remark 1: The infinite sum of (8) converges always.

Proof: By examining the argument $x \left(\prod_{k=1}^{\mathcal{K}} \mathcal{A}_{k,i_k}(x) \right)$ in (8), it holds that $\lim_{x \rightarrow \infty} \mathcal{A}_{k,1}(x) = \lim_{x \rightarrow \infty} (\mathcal{I}_{P_{\text{suc}_k}(\gamma_{\text{S}})}(\mathcal{G}, x - \mathcal{G})) = 1$ and $\lim_{x \rightarrow \infty} x \mathcal{A}_{k,2}(x) =$

$\lim_{x \rightarrow \infty} x (P_{\text{suc}_k}(\gamma_{\text{S}}))^{\mathcal{G}} (1 - P_{\text{suc}_k}(\gamma_{\text{S}}))^{x-\mathcal{G}} / ((x - \mathcal{G}) \text{B}(\mathcal{G}, x - \mathcal{G})) = 0$ since $P_{\text{suc}_k}(\gamma_{\text{S}}) \in [0, 1]$. Hence, the infinite sum converges always. ■

E. Performance trends of the CDF $F_{T_{\text{FCB}}}(t_{\text{FC}}, \mathcal{G})$

In the present section we investigate the impact of crucial network parameters on the performance trends of $F_{T_{\text{FCB}}}(t_{\text{FC}}, \mathcal{G})$. Particularly, Propositions 1, 2 and 3 study the behavior of $F_{T_{\text{FCB}}}(t_{\text{FC}}, \mathcal{G})$ with respect to \mathcal{G} , \mathcal{K} , and P_{P} .

Proposition 1: $F_{T_{\text{FCB}}}(t_{\text{FC}}, \mathcal{G})$ is a monotonic decreasing function with respect to the number of packets \mathcal{G} .

Proof: The proof is given below:

$$F_{T_{\text{FCB}}}(t_{\text{FC}}, \mathcal{G}) \stackrel{(a)}{=} \prod_{k=1}^{\mathcal{K}} \left[\mathcal{I}_{P_{\text{suc}_k}(\gamma)}(\mathcal{G} + 1, t_{\text{FC}} - \mathcal{G}) \right. \\ \left. + (P_{\text{suc}_k}(\gamma))^{\mathcal{G}} (1 - P_{\text{suc}_k}(\gamma))^{t_{\text{FC}} - \mathcal{G}} / (\mathcal{G} \text{B}(\mathcal{G}, t_{\text{FC}} - \mathcal{G} + 1)) \right] \\ > \prod_{k=1}^{\mathcal{K}} \mathcal{I}_{P_{\text{suc}_k}(\gamma)}(\mathcal{G} + 1, t_{\text{FC}} - \mathcal{G}) = F_{T_{\text{FCB}}}(t_{\text{FC}}, \mathcal{G} + 1), \quad (9)$$

where (a) is obtained by using [9, 8.17.18]. Q.E.D. ■

Proposition 2: $F_{T_{\text{FCB}}}(t_{\text{FC}}, \mathcal{G})$ with respect to P_{P} is a piece-wise function. Particularly, for $P_{\text{P}} < P_{\text{con},1} = \gamma_{\text{P}} \sigma_{\text{P}}^2 / (\Omega_{\text{PT,PR}} (-\log(1-v)))$, $F_{T_{\text{FCB}}}(t_{\text{FC}}, \mathcal{G})$ is constant and equal to zero, i.e., $F_{T_{\text{FCB}}}(t_{\text{FC}}, \mathcal{G}) = 0$. $F_{T_{\text{FCB}}}$ increases then monotonically for $P_{\text{con},1} < P_{\text{P}} < P_{\text{con},2}$ and finally, $F_{T_{\text{FCB}}}$ is a decreasing function of P_{P} for $P_{\text{P}} > P_{\text{con},2}$. $P_{\text{con},2}$ is given in (19).

Proof: The proof is available in Appendix D. ■

According to Proposition 2, it holds that if $P_{\text{max}} \rightarrow \infty$, then $F_{T_{\text{FCB}}}(t_{\text{FC}}, \mathcal{G})$ increases proportionally to the value of P_{P} . Hence, increasing the value of P_{P} benefits both the primary and the secondary network.

Proposition 3: $F_{T_{\text{FCB}}}(t_{\text{FC}}, \mathcal{G})$ decreases with the number of SRs \mathcal{K} .

Proof: This holds from the definition of $F_{T_{\text{FCB}}}(t_{\text{FC}}, \mathcal{G})$ in (7), since the product of numbers which are less than 1 decreases with the number of multipliers. ■

In the following, the expectation and the CDF of the number of required clock cycles under the UB scheme is provided, as a benchmark for the comparison with the FCB scheme.

F. CDF of clock cycles required for broadcasting under UB

Under the UB scheme, its CDF denoted by $F_{T_{\text{UB}}}(t_{\text{UB}}, \mathcal{G})$ is given by

$$F_{T_{\text{UB}}}(t_{\text{UB}}, \mathcal{G}) = \Pr \{ T_{\text{UB}} \leq t_{\text{UB}} \} = \sum_{i=\mathcal{G}}^{t_{\text{UB}}} \sum_{w_1=1}^{i-\mathcal{G}+1} \cdots \\ \sum_{w_{\mathcal{G}-1}=1}^{i-\sum_{o=1}^{\mathcal{G}-2} w_o - 1} \left(\prod_{z=1}^{\mathcal{G}-1} \mathcal{V}(w_z) \right) \mathcal{V} \left(i - \sum_{z=1}^{\mathcal{G}-1} w_z \right), \quad (10)$$

where $\mathcal{V}(x) = \prod_{k=1}^{\mathcal{K}} (1 - (1 - P_{\text{suc}_k}(\gamma_{\text{S}}))^x) - \prod_{k=1}^{\mathcal{K}} (1 - (1 - P_{\text{suc}_k}(\gamma_{\text{S}}))^{x-1})$.

Proof: The proof is available in Appendix E. ■

G. Mean of clock cycles required for broadcasting under UB

The average number of needed clock cycles for broadcasting \mathcal{G} packets under UB is denoted by $\mathcal{E}_{\text{UB}}(\mathcal{G})$ and is given by

$$\mathcal{E}_{\text{UB}}(\mathcal{G}) = \mathbb{E} \{ T_{\text{UB}} \} \stackrel{(a)}{=} \mathcal{G} \mathcal{E}_{\text{UB}}(1) \\ = \mathcal{G} \sum_{x=1}^{\infty} x (\mathcal{V}(x) - \mathcal{V}(x-1)), \quad (11)$$

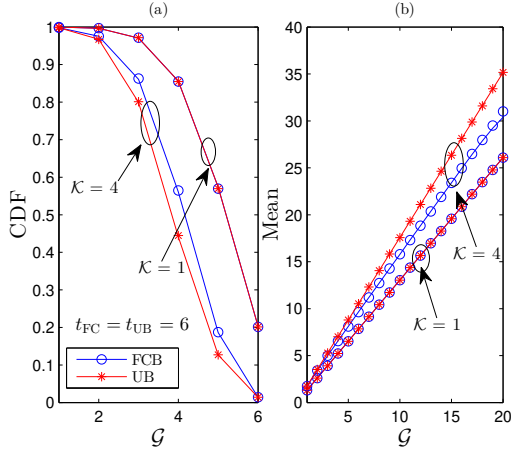


Fig. 2. CDF (a) and expectation (b) of FCB and UB protocols vs. \mathcal{G} packets. Solid lines are plotted from (7), (10), (8) and (11). Markers are Monte-Carlo simulations.

where (a) holds due to the fact that the packets are independent under the uncoded broadcast scheme.

H. Energy efficiency of the secondary networks

Energy efficiency (EE) is defined as the ratio between spectral efficiency and the power consumption of the whole network. Under the considered network, the EE (measured in packets/Joule) under the $x \in \{\text{FCB}, \text{UB}\}$ scheme is defined as follows [10]:

$$\text{EE}_x = (\mathcal{G}/\mathcal{E}_x(\mathcal{G})) / (P_S + P_{\text{circ}}), \quad (12)$$

where P_{circ} is the static power of the ST including all processing power except for the transmit power.

IV. NUMERICAL RESULTS

In this section, numerical results are provided to verify the accuracy of the proposed mathematical framework. Without loss of generality, the following setup is used in this section: $\mathcal{K} = 4$; $R_P = R_S = 0.75$ bits/s/Hz; $P_P = 15$ dBm; NF = 10 dB; Bw = 10 MHz; $\mathcal{G} = 4$ packets; $\eta = 2.75$; $f_c = 1.8$ GHz; $v = 0.1$; $P_{\text{max}} = 25$ dBm; $P_{\text{cir}} = 4.8$ Watt, $\lambda_{u,v} = \lambda = 1$, $\forall u, v$; the positions of ST, PT and PR are (0, 0), (40, 40) and (60, 40), respectively; and the positions of 4 SRs are (60, 0), (25, 25), (-30, 0) and (-30, 10). The number of terms for computing the infinity series is 40.

Fig. 2 plots the $F_{T_{\text{FCB}}}(t_{\text{FC}}, \mathcal{G})$, $F_{T_{\text{UB}}}(t_{\text{UB}}, \mathcal{G})$ (a) and $\mathcal{E}_{\text{FCB}}(\mathcal{G})$, $\mathcal{E}_{\text{UB}}(\mathcal{G})$ (b) versus the number of packets \mathcal{G} . Evidently, the accuracy of the proposed mathematical framework is verified by the Monte-Carlo simulations. In Fig. 2(a), increasing \mathcal{G} decreases $F_{T_{\text{FCB}}}(t_{\text{FC}}, \mathcal{G})$ as demonstrated by Proposition 1. The similar trend also applies to $F_{T_{\text{UB}}}(t_{\text{UB}}, \mathcal{G})$. Additionally, we see that for $\mathcal{K} = 4$ the FCB scheme outperforms the UB scheme for $t_{\text{FC}} = t_{\text{UB}}$ clock cycles. Moreover, the performance of the two schemes is exactly the same when $\mathcal{K} = 1$. Furthermore, this figure also substantiates Proposition 3 according to which the CDF decreases as \mathcal{K} increases. Looking at Fig. 2(b), we notice again that for $\mathcal{K} = 1$ $\mathcal{E}_{\text{FCB}}(\mathcal{G}) = \mathcal{E}_{\text{UB}}(\mathcal{G})$ regardless of \mathcal{G} and that for $\mathcal{K} = 4$, $\mathcal{E}_{\text{FCB}}(\mathcal{G})$ is lower and therefore better than $\mathcal{E}_{\text{UB}}(\mathcal{G})$.

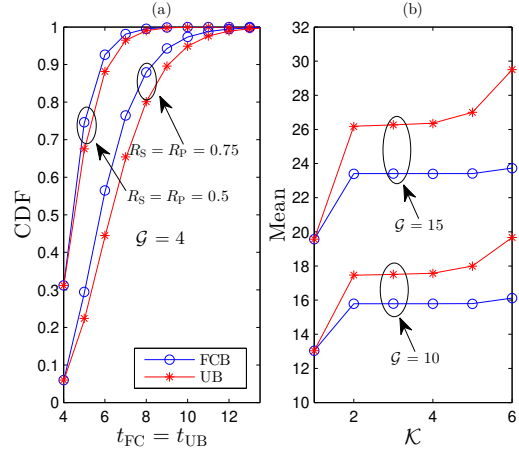


Fig. 3. CDF vs. $t_{\text{FC}} = t_{\text{UB}}$ (a) and mean vs. \mathcal{K} users. The position of the 5th and 6th SRs are (40, -10) and (0, 60). Solid lines are plotted from (7), (10), (8) and (11). Markers are Monte-Carlo simulations.

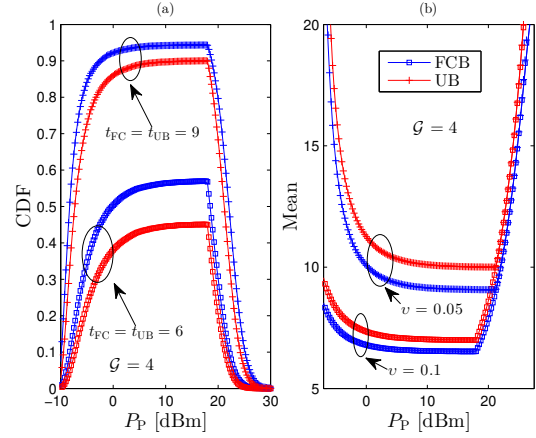


Fig. 4. CDF and mean of FCB and UB vs. P_P [dBm]. Solid lines are plotted from (7), (10), (8) and (11). Markers are Monte-Carlo simulations.

Additionally, the larger the number of packets \mathcal{G} is, the larger the average number of the required clock cycles.

Fig. 3 demonstrates (a) the behaviors of the CDFs of the two protocols with respect to $t_{\text{FC}} = t_{\text{UB}}$ and (b) the average number of required clock cycle for a different number of users \mathcal{K} . Particularly, Fig. 3(a) shows that as the number of required clock cycles t_{FC} increases so does the CDF. Fig. 3(a) also reveals that the higher the expected rate the smaller the CDF. More precisely, the curve of FCB scheme under $R_S = 0.5$ bits/s/Hz is above 0.9 at $t_{\text{FC}} = 6$ while the CDF of the same scheme under $R_S = 0.75$ bits/s/Hz is only around 0.55. This behavior holds also in the case of the UB scheme. Fig. 3(b) unveils the trends of the $\mathcal{E}_{\text{FCB}}(\mathcal{G})$ and $\mathcal{E}_{\text{UB}}(\mathcal{G})$ with respect to \mathcal{K} for different values of \mathcal{G} . In particular, it verifies the conclusion drawn already from Fig. 2 that increasing \mathcal{K} increases the average number of required clock cycles. Additionally, the gap between the two schemes for the current setup is around 2 clock cycles which is considerable.

Fig. 4 demonstrates the behavior of both the CDF and the mean with respect to P_P . Fig. 4(a), confirms the finding of Proposition 2 that the CDFs of both schemes are first equal to zero, followed by a monotonic increase and then monotonic decrease until zero as P_P increases from -10 to 30 dBm.

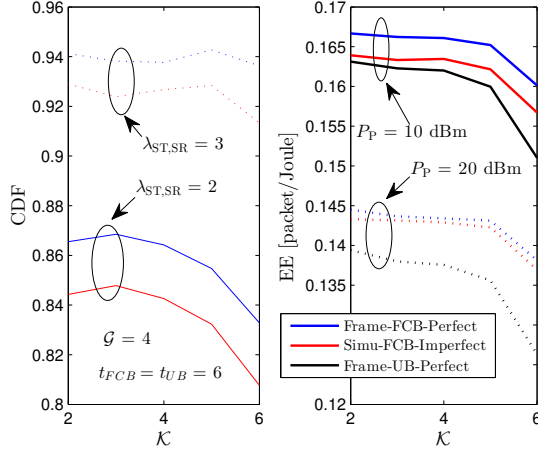


Fig. 5. CDF and EE vs. \mathcal{K} . Blue and black curves are given by (7), (10), and (12) under perfect CSI at the secondary network, whereas the red curves are Monte-Carlo simulations under imperfect CSI at the secondary network.

The maximum value of the CDF is that of Fig. 3(a) for the corresponding value of t_{FC} . Fig. 4(a) demonstrates that the FCB scheme always outperforms the UB scheme regardless of the value of P_P . Fig. 4(b) demonstrates that, as expected, when the CDF of clock cycles required for broadcasting tends to zero in Fig. 4(a) the respective average number of expected clock cycles tends to infinity.

Fig. 5 unveils the performance of the CDF and EE as a function of \mathcal{K} under both perfect and imperfect CSI. Particularly, the following imperfect CSI model is considered. Channel coefficients at PR and SRs from ST are assumed to be imperfect and are modelled by [12]: $\tilde{h}_{ST,v} = \rho h_{ST,v} + \sqrt{1 - \rho^2} w_{ST,v}$, $\forall v$, where $\tilde{h}_{ST,v}$ is the estimate of $h_{ST,v}$ while $w_{ST,v}$ is a complex Gaussian RV with zero mean and the same variance as $h_{ST,v}$. $\rho \in [0, 1]$ is the correlation coefficient and is calculated by $J_0(2\pi f_d \tau)$, where $J_0(\cdot)$ is the zeroth-order Bessel function of the first kind, $f_d = v_e \cos(\alpha) f_c / c$ is the Doppler shift, v_e is the relative velocity of SRs, α is the angle between wave propagation and motion direction, and τ is the feedback delay. In the current work, we choose $v_e = 80$ km/h, $\alpha = 60^\circ$ and $\tau = 1$ ms. We observe again that the CDF monotonically decreases with \mathcal{K} and the gap between the perfect and imperfect CSI is minor, i.e., ≤ 0.02 , for both CDF and EE with different value of P_P and channel gain $\lambda_{ST,SRs}$. Additionally, the impact of the imperfect CSI can be effectively mitigated by either increasing the channel gain $\lambda_{ST,SRs}$ or P_P . The behavior of the EE vs. \mathcal{K} is illustrated in Fig. 5(b). We see that the EE even under the imperfect CSI is still higher than the UB scheme. Additionally, increasing P_P scales down the EE, since the denominator of the EE increases faster than the numerator when P_P increases.

V. CONCLUSION

The closed-form expressions of the CDF, the expectation, and the EE of the broadcasting in CRNs with FC were derived in the present letter. We also examined the trends of the CDF with respect to key network parameters, allowing for the optimization of those parameters by the network operator. Our

findings revealed that the CDF is monotonically decreasing function with respect to \mathcal{G} and \mathcal{K} . Regarding the impact of the P_P , the CDF increases and then decreases, revealing its maximal value. Additionally, the performance of the proposed framework was compared versus that of the typical UB scheme, while numerical results illustrated the superior performance of the FCB scheme over the UB broadcast scheme and corroborated the accuracy of our performance analysis. The current work can be extended in several directions. One of the promising ways is to consider multiple STs to further enhance system performance. Another technique is to apply advanced frequency reuse and clustering to ameliorate the performance of the whole network. Besides, jointly studying the performance of the PN and SN is also an interesting topic to address in the future. Multi-hop transmission is another favorable extension to boost the system's reliability by shortening the transmission distance. Finally, tools from stochastic geometry can be applied to better capture the randomness of the nodes' positions in CRNs [10].

APPENDIX

A. Proof of Eq. (4)

The derivation of (4) is given in this section, let us first formulate the definition of random variable Z as follows:

$$\begin{aligned} \overline{F}_Z(z) &= \Pr \{ aX / (c + bY) \geq z \} \\ &= \int_{y=0}^{\infty} \int_{x=z(c+by)/a}^{\infty} f_{X,Y}(x, y) dx dy \\ &\stackrel{(a)}{=} \int_{y=0}^{\infty} \exp(-z(c+by)/(a\omega_X)) f_Y(y) dy \\ &\stackrel{(b)}{=} \frac{1}{\omega_Y} \exp\left(-\frac{zc}{a\omega_X}\right) \int_{y=0}^{\infty} \exp\left(-y\left(\frac{bz}{a\omega_X} + \frac{1}{\omega_Y}\right)\right) dy \\ &= \exp(-zc/(a\omega_X)) (1 + zb\omega_Y/(a\omega_X))^{-1}, \end{aligned} \quad (13)$$

where (a) holds by substituting the complementary CDF and probability density function (PDF) of exponential RVs X , Y and applying the independence property of X and Y ; (b) holds by employing the PDF of the exponential distribution. Q.E.D.

B. Proof of Eq. (5)

To identify the transmit power of ST we first derive the OP of the primary receiver PR denoted by $OP_{PR}(\gamma_P)$ as follows:

$$\begin{aligned} OP_{PR}(\gamma_P) &= \Pr \{ SINR_{PR} \leq \gamma_P \} \\ &= \int_{|h_{ST,PR}|^2=y=0}^{\infty} \int_{|h_{PT,PR}|^2=x=q(y)}^{\infty} f_{|h_{PT,PR}|^2, |h_{ST,PR}|^2}(x, y) dx dy \\ &\stackrel{(a)}{=} 1 - \exp(-\gamma_P \sigma_P^2 / (\Omega_{PT,PR} P_P)) (1 + \gamma_P \Omega_{ST,PR} P_S / (\Omega_{PT,PR} P_P))^{-1}. \end{aligned} \quad (14)$$

Here $q(y) = \gamma_P (\sigma_P^2 + P_S \Omega_{ST,PR} y) / (P_P \Omega_{PT,PR})$, $SINR_{PR} = P_P \Omega_{PT,PR} |h_{PT,PR}|^2 / (\sigma_P^2 + P_S \Omega_{ST,PR} |h_{ST,PR}|^2)$ and (a) is obtained immediately with the help of Lemma 1 since the integration is similar as in Lemma 1. Next, substituting OP_{PR} in (14) for the OP's condition, we get the P_{adp} as follows:

$$\begin{aligned} OP_{PR}(\gamma_P) \leq v &\Leftrightarrow P_{adp} \leq \Omega_{PT,PR} P_P / (\Omega_{ST,PR} \gamma_P) \\ &\times \left(\exp(-\gamma_P \sigma_P^2 / (\Omega_{PT,PR} P_P)) (1 - v)^{-1} - 1 \right). \end{aligned} \quad (15)$$

Finally, by substituting P_{adp} into (5) we obtain P_S . Q.E.D.

C. Proof of Eq. (7)

$$\begin{aligned} F_{T_{\text{FCB}}}(t_{\text{FC}}, \mathcal{G}) &= \Pr \{T_{\text{FCB}} \leq t_{\text{FC}}\} \stackrel{(a)}{=} \prod_{k=1}^{\mathcal{K}} \Pr \{t_k \leq t_{\text{FC}}\} \\ &\stackrel{(b)}{=} \prod_{k=1}^{\mathcal{K}} \sum_{i=\mathcal{G}}^{t_{\text{FC}}} \binom{i-1}{\mathcal{G}-1} (P_{\text{suc}_k}(\gamma_S))^{\mathcal{G}} (1 - P_{\text{suc}_k}(\gamma_S))^{i-\mathcal{G}} \\ &= \prod_{k=1}^{\mathcal{K}} \mathcal{I}_{P_{\text{suc}_k}(\gamma_S)}(\mathcal{G}, t_{\text{FC}} - \mathcal{G} + 1), \end{aligned} \quad (16)$$

where (a) is obtained due to the fact that the success probabilities of all STs are independent to each other; t_k is the RV of the number of required clock cycles to receive \mathcal{G} packets by the k -th SRs; (b) holds by employing the definition of binomial distribution with success probability $P_{\text{suc}_k}(\gamma_S)$ provided in (6); and the last equation is obtained by employing [9, Eq. 8.17.5]. Q.E.D.

D. Proof of Proposition 2

To investigate the behaviour of the CDF of T_{FCB} with respect to P_P , let us take the first-order derivative of $F_{T_{\text{FCB}}}(t_{\text{FC}}, \mathcal{G})$ with respect to P_P as follows:

$$\begin{aligned} \dot{F}_{T_{\text{FCB}}}(P_P = x) &= dF_{T_{\text{FCB}}}(t_{\text{FC}}, \mathcal{G}, P_P = x) / dx \\ &= \sum_{k=1}^{\mathcal{K}} \dot{\mathcal{I}}_{P_{\text{suc}_k}(\gamma_S, x)}(\mathcal{G}, t_{\text{FC}} - \mathcal{G} + 1) \\ &\quad \times \prod_{\bar{k} \neq k=1}^{\mathcal{K}} \mathcal{I}_{P_{\text{suc}_{\bar{k}}}(\gamma_S, x)}(\mathcal{G}, t_{\text{FC}} - \mathcal{G} + 1), \end{aligned} \quad (17)$$

where $\dot{f}(x) = df(x)/dx$ is the first-order derivative of f over x ; the first derivative of $\mathcal{I}_{P_{\text{suc}_k}(\gamma_S, x)}(\mathcal{G}, t_{\text{FC}} - \mathcal{G} + 1)$ with respect to $x = P_P$ is given by

$$\begin{aligned} \dot{\mathcal{I}}_{P_{\text{suc}_k}(\gamma_S, x)}(\mathcal{G}, t_{\text{FC}} - \mathcal{G} + 1) &\stackrel{(a)}{=} \dot{P}_{\text{suc}_k}(\gamma_S, x) (P_{\text{suc}_k}(\gamma_S, x))^{\mathcal{G}-1} \\ &\quad \times (1 - P_{\text{suc}_k}(\gamma_S, x))^{t_{\text{FC}} - \mathcal{G}} / \mathbf{B}(\mathcal{G}, t_{\text{FC}} - \mathcal{G} + 1), \\ \dot{P}_{\text{suc}_k}(\gamma_S, x) &= \begin{cases} 0 & 0 < P_P < P_{\text{con},1} \\ v_k(x) > 0 & P_{\text{con},1} < P_P < P_{\text{con},2} \\ r_k(x) < 0 & P_P > P_{\text{con},2} \vee P_P = 0 \end{cases}, \end{aligned} \quad (18)$$

where $v_k(x) = \left((u(x))^{-2} \right) \exp(-C_{1,k}/u(x)) \times \left[C_{1,k} \dot{u}(x) (1 + C_{2,k}/u(x))^{-1} - C_{2,k} (u(x) - x \dot{u}(x)) \times (1 + x C_{2,k}/u(x))^{-2} \right] > 0$; $\dot{u}(x) = \left[C_4 \exp(-C_3/x) (1 - v)^{-1} (1 + C_3/x) - 1 \right] > 0$; $u(x) - x \dot{u}(x) = -C_3 C_4 \exp(-C_3/x) (1 - v)^{-1} < 0$; $r_k(x) = -(C_{2,k}/P_{\text{max}}) \exp(-C_{1,k}/P_{\text{max}}) (1 + C_{2,k}x/P_{\text{max}})^{-2} < 0$; (a) holds with the help of [11] and due to the fact that $F_{T_{\text{FCB}}}(t_{\text{FC}}, \mathcal{G})$ solely depends on P_P via P_{suc} ; $P_{\text{con},1}$ is given in Proposition 2. $\dot{P}_{\text{suc}_k}(\gamma_S, x)$ in (18) is a piece-wise function of P_P since P_S is a piece-wise function of P_P . $P_{\text{suc}_k}(\gamma_S, x)$ is continuous but not differentiable at $P_P = P_{\text{con},2}$ that is the root of the following non-linear equation

$$\exp(-C_3/P_P) (1 - v)^{-1} - 1 = P_{\text{max}} / (C_4 P_P). \quad (19)$$

In (19), we observe that $P_{\text{con},2}$ is a unique root since the right hand side (RHS) is monotonically decreasing function from infinity to zero while the left hand side (LHS) is monotonically

increasing function from -1 to $(1 - v)^{-1} - 1 > 0, v \in (0, 1]$ when P_P goes from zero to infinity. As a result, the LHS only crosses the RHS at one single point and this is also the root of the equation. From (17) and (18), we prove the statement of Proposition 2 and close the proof here.

E. Proof of Eq. (10)

The derivation of the CDF of the UB scheme is provided in this section. Let us begin with the definition of the CDF that is given by:

$$\begin{aligned} F_{T_{\text{UB}}}(t_{\text{UB}}) &= \Pr \{T_{\text{UB}} \leq t_{\text{UB}}\} = \Pr \left\{ \sum_{z=1}^{\mathcal{G}} u_z = i \right\} \\ &\stackrel{(a)}{=} \sum_{i=\mathcal{G}}^{t_{\text{UB}}} \sum_{w_1=1}^{i-\mathcal{G}+1} \dots \sum_{w_{\mathcal{G}-1}=1}^{i-\sum_{o=1}^{\mathcal{G}-2} w_o-1} \left(\prod_{z=1}^{\mathcal{G}-1} \Pr \{u_z = w_z\} \right) \\ &\quad \times \Pr \left\{ u_{\mathcal{G}} = i - \sum_{z=1}^{\mathcal{G}-1} w_z \right\}, \end{aligned} \quad (20)$$

where (a) holds by considering all combinations of w_z ; u_z , $z \in \{1, \dots, \mathcal{G}\}$, is an independent identically distributed (i.i.d.) RV corresponding to the maximal number of required clock cycles for the \mathcal{K} SRs to successfully receive the z -th packet. So,

$$\Pr \{u_z = \max_{k \in \{1, \mathcal{K}\}} \{s_k\} = w_z\} \stackrel{(a)}{=} \mathcal{V}(w_z), \quad (21)$$

where s_k is the number of clock cycles required for the k -th SR to decode one packet; (a) holds due to the fact that s_k follows a geometric distribution whose CDF is given by $F_{s_k}(a) = 1 - (1 - P_{\text{suc}_k}(\gamma_S))^a$, where a is the number of trials; the probability mass function (PMF) of u_z is then computed as $p_{u_z}(w_z) = \mathcal{V}(w_z)$. Finally, substituting (21) into (20) we obtain (10) and close the proof here.

REFERENCES

- [1] S. K. Sharma *et al.*, "Cognitive Radio Techniques Under Practical Imperfections: A Survey," *IEEE Commun. Surveys Tuts.*, vol. 17, no. 4, pp. 1858-1884, 2015.
- [2] Z. Zheng *et al.*, "Performance Analysis of Fountain Coded Non-Orthogonal Multiple Access With Finite Blocklength," *IEEE Wireless Commun. Lett.*, vol. 10, no. 8, pp. 1752-1756, Aug. 2021.
- [3] X. Chen *et al.*, "Efficient Resource Allocation in a Rateless-Coded MUMIMO Cognitive Radio Network With QoS Provisioning and Limited Feedback," *IEEE Trans. Veh. Technol.*, vol. 62, no. 1, pp. 395-399, Jan. 2013.
- [4] X. Wang *et al.*, "ARCOR: Agile Rateless Coded Relaying for Cognitive Radios," *IEEE Trans. Veh. Technol.*, vol. 60, no. 6, pp. 2777-2789, Jul. 2011.
- [5] B. Rashid *et al.*, "Broadcasting strategies for cognitive radio networks: Taxonomy, issues, and open challenges," *Comput. Electr. Eng.*, vol. 52, pp. 349-361, 2016.
- [6] L. T. Tu *et al.*, "On the Energy Efficiency of Heterogeneous Cellular Networks With Renewable Energy Sources—A Stochastic Geometry Framework," *IEEE Trans. Wireless Commun.*, vol. 19, no. 10, pp. 6752-6770, Oct. 2020.
- [7] T. Ahrendt, "Fast Computations of the Exponential Function," *STACS 1999 Lecture Notes in Computer Science*, vol 1563, 1999.
- [8] I. S. Gradshteyn *et al.*, "Table of integrals, series, and products," 7th edition Elsevier/Academic Press, 2007.
- [9] NIST Digital Library of Mathematical Functions. <http://dlmf.nist.gov/>, Release 1.1.2 of 2021-06-15.
- [10] M. Di Renzo *et al.*, "System-Level Modeling and Optimization of the Energy Efficiency in Cellular Networks—A Stochastic Geometry Framework," *IEEE Trans. Wireless Commun.*, vol. 17, no. 4, pp. 2539-2556, Apr. 2018.
- [11] Wolfram, [Online] "<https://functions.wolfram.com/06.21.02.0001.01>".
- [12] H. A. Suraweera *et al.*, "Capacity Limits and Performance Analysis of Cognitive Radio With Imperfect Channel Knowledge," *IEEE Trans. on Veh. Technol.*, vol. 59, no. 4, pp. 1811-1822, May 2010.